Forest Ecology and Management 542 (2023) 121113

Contents lists available at ScienceDirect

Forest Ecology and Management

journal homepage: www.elsevier.com/locate/foreco

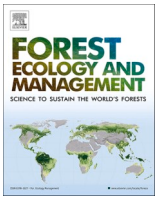

Functional traits underlie specialist-generalist strategies in whitebark pine and limber pine

Danielle E.M. Ulrich [a,*], Chloe Wasteneys [a], Sean Hoy-Skubik [a], Franklin Alongi [b]

[a] Ecology Department, Montana State University, Bozeman, MT 59717, USA
[b] Plant Sciences and Pathology Department, Montana State University, Bozeman, MT 59717, USA

ARTICLE INFO

Keywords:
Biomass allocation
Budburst phenology
High-light tolerance
Physiology
Seedling traits
Stomata
Water relations

ABSTRACT

Plant species life history strategies are described by functional variation spanning an acquisitive and conservative resource use continuum. Specialist species can exhibit traits promoting one end of the continuum, while generalist species can display traits promoting both acquisitive and conservative resource use. Whitebark pine (*Pinus albicaulis,* PIAL) and limber pine (*Pinus flexilis,* PIFL) are two high-elevation pines that have similar growth and morphology, yet contrasting elevational distributions with PIAL viewed as a specialist inhabiting a narrower elevation range, and PIFL as a generalist inhabiting a broader elevation range. We compared the physiological and morphological traits of greenhouse-grown 5-year-old PIAL and PIFL. Our results suggest that PIFL's acquisitive and conservative resource use traits contribute to its generalist strategy and ability to inhabit a greater range of elevations than PIAL. PIFL had greater acquisitive resource use traits including: high-light tolerance (greater Q_{sat}, greater fascicle density), increased biomass allocation to photosynthetic tissue (higher needle biomass, aboveground:belowground biomass, needle:branch + stem biomass), and higher C and water uptake (greater stomatal density and size, higher C assimilation rate), as well as greater conservative resource use traits including: greater physical stress resistance (shorter height, higher stem and branch diameters, greater branch and stem diameter:length), drought tolerance (higher SWC, leaf starch proportion), and drought avoidance (earlier budburst phenology, smaller hydroscape area) than PIAL. Our results suggest that PIFL may make more efficient use of high-light loads and maximize C and water uptake when moisture is abundant during spring snowmelt before the onset of dry summer conditions. Other conservative resource use traits describing cold tolerance, heat tolerance, and drought tolerance did not differ between species, suggesting that both species exhibit traits that promote similar conservative resource use enabling their overlapping persistence at higher elevations. Comparing the physiology of PIAL and PIFL within the same environment enables us to identify physiological mechanisms that underlie species establishment and survival, and how juvenile physiology contributes to their contrasting distributions and their generalist-specialist strategies.

1. Introduction

Given the rapid pace of climate change, it remains challenging to predict how environmental change will affect forest species' distributions, ecosystem functions, and vegetation-climate feedbacks (Adams et al., 2010; Monahan et al., 2013). In the western US, exceptionally warm, dry conditions have resulted in widespread forest mortality and migration of tree species, resulting in shifts in species' geographic distributions (Allen et al., 2010; "IPCC," 2018). To improve our ability to understand and predict climate change effects on tree species distributions, research generally has examined physiological mechanisms of adult tree mortality (Keane et al., 2017), rather than mechanisms that underlie establishment and survival of younger developmental stages (Vogan and Schoettle, 2015). The ability of tree species to migrate and regenerate (naturally or assisted) depends on the successful establishment of seedlings that survive into juveniles and, ultimately, into reproductively mature adults. A challenge to tree species migration and regeneration is that younger developmental stages are more vulnerable to abiotic and biotic stressors than mature adult life stages, creating a bottleneck to shifts in species distributions under changing climates. Our understanding of species distribution drivers is limited because predictions are often based on a species' current distribution alone,

* Corresponding author at: Montana State University – Ecology, 310 Lewis Hall, Bozeman, MT 59717, USA.
E-mail address: Danielle.Ulrich@montana.edu (D.E.M. Ulrich).

https://doi.org/10.1016/j.foreco.2023.121113
Received 22 March 2023; Received in revised form 11 May 2023; Accepted 13 May 2023
Available online 19 May 2023
0378-1127/© 2023 Elsevier B.V. All rights reserved.

ignoring that drivers of adult tree survival may differ from those governing juvenile survival. Therefore, we need to better examine juvenile physiological mechanisms of establishment and survival to improve our understanding of how species distributions will be affected by changing climates.

Physiological mechanisms underlying juvenile survival and fitness include a seedling's ability to take up carbon dioxide (CO_2), water, and photosynthetically active radiation (PAR) for photosynthesis, and subsequently growth and resistance to abiotic and biotic stresses (Johnson et al., 2011). These mechanisms are manifested in traits which affect morphology (e.g., crown architecture, stomatal arrangements, biomass allocation) and physiology (e.g., photosynthetic capacity or tolerance to drought, heat, cold). Diverse combinations of these morphological and physiological traits enable an individual to establish and persist in a given environment, contributing to its species' geographic distribution (Savolainen et al., 2007). Therefore, comparing traits between species can reveal mechanisms of establishment and survival and their contribution to species' geographic distributions, especially in marginal high-elevation environments (Germino and Smith 1999).

Certain combinations of such traits underlie life history survival strategies that span a continuum from acquisitive to conservative strategies of resource use (Reich, 2014; Wright et al., 2004). Specialist species that inhabit a narrow range of environments display either acquisitive ("fast") or conservative ("slow") extremes of the resource use continuum. In contrast, generalist species that inhabit a broader range of environments have displayed the entire range of variation between both acquisitive and conservative extremes of the resource use continuum (Sanaphre-Villanueva et al., 2017). The classification of generalist versus specialist is important because generalist species adapted to heterogeneous climates may fare better under changing climates than specialist species (Ackerly et al., 2010). However, we do not fully understand the physiological mechanisms contributing to such generalist and specialist strategies.

Whitebark pine (*Pinus albicaulis* Englem., PIAL) and limber pine (*Pinus flexilis* James., PIFL) are two high-elevation five-needle white pine species (Family Pinaceae, Genus *Pinus*, subgenus *Strobus* (Gernandt et al., 2005)) that have broad, overlapping geographic distributions in western North America (Fig. 1). However, PIAL and PIFL differ in their elevational distribution limits (Supporting Figure S1) with PIAL being viewed as a specialist and PIFL a generalist (Hankin and Bisbing, 2021; Tomback et al., 2011), and PIAL's distribution extending more northward than PIFL's. PIAL exists within narrower elevational bands, inhabiting the upper subalpine to upper treeline (1600–3660 m) (Arno, 1989), consistent with its distribution extending the farthest northward of any North American pine (Tomback et al., 2011). In contrast, PIFL has a broader elevational range than PIAL, occurring at lower elevations from lower treeline to upper treeline (870–3810 m) (Steele, 1990) and more arid regions (Tomback et al., 2011). However, of the studies that have investigated the juvenile physiology of these species (Borgman et al., 2015; Jacobs and Weaver, 1990; Mahalovich et al., 2016; Reinhardt et al., 2011; Vogan and Schoettle, 2015), none have compared the physiology between species grown in the same environment. Therefore,

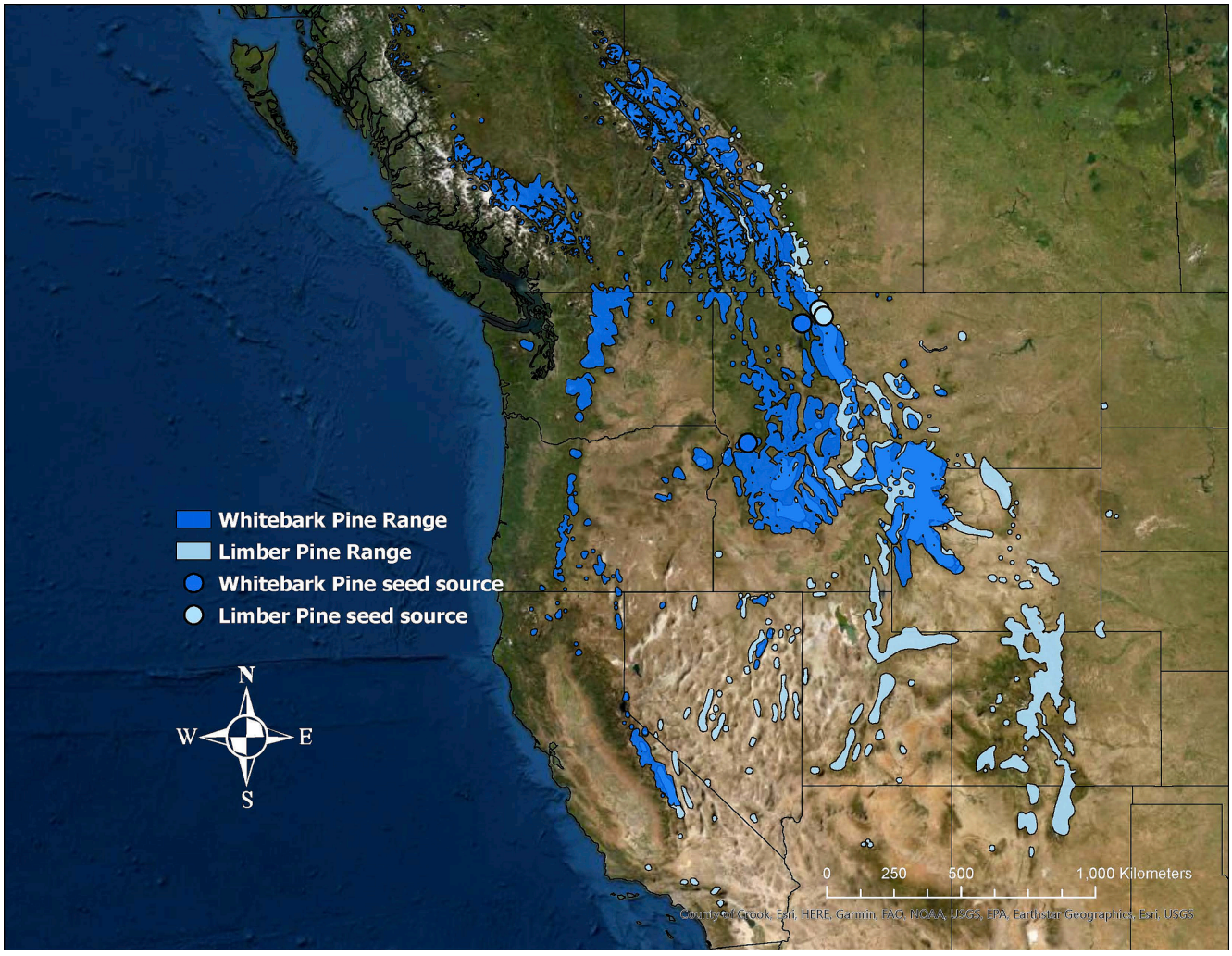

Fig. 1. Species distributions of whitebark pine (dark, PIAL) and limber pine (light, PIFL), and seed source location of each family per species (circles) (Table 1).

we do not understand the physiological mechanisms contributing to PIFL and PIAL being viewed as generalist and specialist, respectively, nor how their distributions are influenced by juvenile physiology (Hansen et al., 2021).

Despite their contrasting distributions, PIAL and PIFL have many similarities, making their comparison useful for identifying physiological mechanisms that may underlie species establishment and survival, the extent to which juvenile physiology contributes to their contrasting distributions, and generalist-specialist strategies to inform management and restoration efforts. Both species are morphologically similar and oftentimes indistinguishable (without mature cones), have a similar growth habit and dispersal mechanism for large seeds, and persist on well-drained nutrient-poor soil. PIAL and PIFL are declining at alarming rates due to changes in climate, white pine blister rust (causal agent *Cronartium ribicola*), and mountain pine beetle (*Dendroctonus ponderosae*) (Cleaver et al., 2017; Goeking and Izlar, 2018). Both species are considered foundation and keystone species, so their decline has far-reaching ecological consequences; their seeds are dispersed and cached by Clark's nutcrackers (*Nucifraga columbiana*), are a high nutrition food source for the threatened grizzly bear (*Ursus arcto*), and their ability to colonize exposed sites provides habitat for other species (Maher et al., 2005). Both PIAL and PIFL have been declared endangered under the Canadian Species at Risk Act (COSEWIC, 2014; 2010). PIAL is now a threatened species under the U.S. Endangered Species Act (ESA) and has the largest range of any tree species listed under the ESA (U.S. Fish and Wildlife Service, 2022). The primary restoration strategy for PIAL is outplanting white pine blister rust-resistant seedlings. This strategy has not been applied to PIFL because mortality is not yet as severe as PIAL's; however, because white pine blister rust is expected to continue to spread throughout PIFL forests (Schoettle and Sniezko, 2007), PIFL may require the same approach of outplanting rust-resistant seedlings in the future. To improve outplanting efforts and our ability to predict climate change effects on species distributions, an understanding of the physiological mechanisms that influence survival, mortality, and growth is critical (Bradley St Clair and Howe, 2007; Chmura et al., 2011).

In this study, we compared physiological and morphological traits (biomass, stomatal traits, budburst phenology, gas exchange, leaf non-structural carbohydrates, C isotope ratios, foliar N content, photosynthetic capacity, and high-light, drought, heat, and cold stress tolerances) of greenhouse-grown 5-year-old PIAL and PIFL. We asked: 1) How do physiological and morphological traits differ between PIAL and PIFL when grown in the same environment? and 2) How do those trait differences relate to their contrasting elevational distributions and their respective generalist-specialist strategies? We hypothesized that PIFL would exhibit traits that enable a generalist strategy (i.e., both acquisitive and conservative resource use traits), allowing it to inhabit a broader range of elevations than PIAL. We expected that both species would exhibit traits that promote conservative resource use enabling their persistence at higher elevations (e.g., tolerance to cold, drought, and heat such as higher leaf mass per area, higher C storage). Also, we expected PIFL (and not PIAL) to exhibit traits promoting acquisitive resource use that enables PIFL's persistence in and higher tolerance to lower elevation environments including: higher light use (increased allocation to photosynthetic tissue, greater high-light tolerance) and higher C and water uptake (higher photosynthetic rate, increased stomatal size and/or density, earlier budburst phenology).

2. Materials and methods

We obtained 5-year-old whitebark pine (PIAL) and limber pine (PIFL) individuals from the US Forest Service Coeur d'Alene (CDA) Nursery, which were grown from seed collected from geolocated parent trees (families) for outplanting efforts (Overton et al., 2016). PIAL originated from four families named: 6184, 6186, 6557, and BD. PIFL originated from two families named: LBP11 and LP07. Average annual climate variables (1991–2020; spatial resolution of 800 m) of each family seed source location were obtained from the PRISM Climate Group ("PRISM," 2018) and included: total annual precipitation (Precip), annual minimum, maximum, and mean temperature (T_{min}, T_{max}, T_{mean}, °C), minimum, maximum, and mean vapor pressure deficit (VPD_{min}, VPD_{max}, VPD_{mean}, hPa), and total daily global shortwave solar radiation received on a horizontal surface averaged over all days in the month (Solar Radiation, MJ m^{-2} day^{-1}) (Table 1).

Bare root seedlings were transplanted to pots (9 cm × 19 cm × 46 cm) with a peat-perlite soil medium (a 4:1 mix of Sunshine Mix #1 (Sungro, Agawam, MA, USA):perlite) and placed in the Plant Growth Center greenhouse at Montana State University, Bozeman, MT, USA in June 2020. During the two growing seasons (Jun-Oct 2020, May-Oct 2021), individuals were watered and fertilized weekly (21 %N, 5 % P2O5, 20 %K2O, 7.18 g L^{-1}). During the winter months (Nov-Apr 2020–2021), fertilizer concentration was reduced to 25% of the growing season amount, and individuals were watered when weekly soil volumetric water content (VWC) reached ~15% (HydroSense II Handheld Soil Moisture Sensor, Campbell Scientific, Logan, UT, USA). Greenhouse conditions during the two growing seasons consisted of a 16-hour photoperiod, 21.1 °C daytime temperature, 18.3 °C nighttime temperature, and average daytime photosynthetically active radiation of 843.0 μmol m^2 s^{-1}. Sample sizes for each trait ranged from 0 to 25 per family per species (Supporting Table S1).

2.1. Morphology, biomass

Morphological traits were measured Jun 2020-Aug 2021 and included: stem base diameter, stem height, stem base diameter:stem height, fascicle density (FD), branch diameter, branch length, branch diameter:branch length, needle width, needle length, the ratio of sunlit leaf area to total leaf area (STAR), leaf mass per area (LMA), and biomass (needle, branch, stem, root, aboveground:belowground). Stem base diameter, stem height, stem base diameter:stem height, and needle width and length were measured with calipers. To determine FD, three first order lateral branches from the terminal stem were randomly selected for measuring branch diameter and branch length with calipers and counting the total number of fascicles on each branch. FD was determined as the number of fascicles divided by branch length. The average of the three branches was used to determine FD, branch diameter, branch length, and branch diameter:branch length. To determine STAR, we determined the sunlit leaf area from a top-down photographic image of the crown using ImageJ (Schneider et al., 2012). We determined fresh total leaf area from a photographic image of all needles (removed from the crown) laid flat using ImageJ. Lower STAR indicates more self-shading and leaf overlap (Germino and Smith, 1999). All needles were then dried for at least 48 h at 50 °C, and subsequently weighed for dry leaf mass. LMA was determined as the ratio of dry leaf mass to fresh total leaf area. Biomass measurements were determined by separating, drying, and weighing needles, branches, stems and roots. Dried needles were ground and analyzed for leaf carbon isotope ratios ($\delta^{13}C$) and leaf N content at the Cornell Stable Isotope Laboratory (Ithaca, NY, USA).

2.2. Stomatal traits

Stomatal traits were measured in Sep 2020-May 2021 and included: stomatal pore size (area), stomatal pore length, stomatal density per needle length, stomatal density per needle area, and stomatal density per volume. Two newest mature, fully expanded needles (2020 foliage) were collected from two separate fascicles, each from the middle of a separate branch. Stomatal prints were taken by applying a coat of clear nail polish to the needle, letting it dry, and then using a piece of cellophane tape to transfer the dried nail polish print onto a microscope slide (Bennett et al., 2018). Stomatal prints were visualized and photographed under a microscope (Micromaster, Fisher Scientific, Hampton,

Table 1
Species (whitebark pine, PIAL; limber pine, PIFL) and family seed source origin location (latitude, longitude, elevation (Elev), Fig. 1) and annual climate ("PRISM," 2018). Total precipitation (Precip), minimum temperature (T_{min}), maximum temperature (T_{max}), mean temperature (T_{mean}), minimum vapor pressure deficit (VPD_{min}), maximum vapor pressure deficit (VPD_{max}), mean vapor pressure deficit (VPD_{mean}), total daily global shortwave solar radiation received on a horizontal surface averaged over all days in the month (Solar radiation).

Species	Family	Latitude	Longitude	Elev m	Precip mm	T_{min} °C	T_{max} °C	T_{mean} °C	VPD_{min} hPa	VPD_{max} hPa	VPD_{mean} hPa	Solar radiation MJ m^{-2} day^{-1}
PIAL	BD	48.326996	−114.045701	1524	1315	−1.5	7.7	3.1	1.5	6.72	4.11	11.84
	6184	48.3266	−114.0475	1524	1304	−1.4	7.8	3.2	1.51	6.81	4.16	11.82
	6186	48.3273	−114.0451	1524	1350	−1.7	7.4	2.9	1.46	6.43	3.945	11.89
	6557	45.5977	−115.8635	2164	1468	−2.9	7.7	2.4	1.74	7.48	4.61	14.14
PIFL	LBP11	48.6314896	−113.4650533	2225	1757	−4.8	5	0.1	1.34	5.47	3.405	13.11
	LP07	48.4911079	−113.3240763	1646	1106	−0.8	8.5	3.9	1.57	7.53	4.55	11.22

New Hampshire, USA) at 100x magnification using a microscope camera (Swiftcam SC1003-CK, Swift Optical Instruments, Shertz, Texas, USA) and Swift Imaging 3.0 software. We measured stomatal traits using ImageJ (Schneider et al., 2012) as follows: stomatal pore area was determined by tracing the outline of each stomata; stomatal pore length was measured as the longest length of each stomata (parallel with needle length); stomatal density per length was determined by dividing the number of stomata per row by row length; stomatal density per area was determined by dividing the total number of stomata in the image by needle area (row length × needle width); and stomatal density per volume was determined by dividing the total number of stomata in the image by volume (row length × needle width × needle width).

2.3. Budburst phenology

We visually assessed budburst phenology weekly during 26 Feb 2021-1 Jul 2021 within six stages of budburst: stage 1 = tight bud, stage 2 = early bud swelling, stage 3 = advanced bud swelling, stage 4 = sheath emergence, stage 5 = needle emergence, and stage 6 = needle elongation (Martínez-Berdeja et al., 2019).

2.4. Physiological traits

Gas exchange measurements of C assimilation (A) and stomatal conductance (g_s) were monitored weekly for 11 weeks (13 Jul-9 Sep 2021) (08 *h*00-12 *h*00) using a portable photosynthesis system equipped with an infrared gas analyzer (LI-6800, Licor, Lincoln, NE USA). Cuvette conditions were set to: 1000 μmol m^{-2} photosynthetic photon flux density (saturating light level in the greenhouse), 60% relative humidity, 400 ppm [CO_2], 25 °C leaf temperature, and 500 μmol s^{-1} flow rate.

Non-structural carbohydrates (NSCs) were measured on needles collected from well-watered individuals ~every 3 weeks for 11 weeks (13 Jul-9 Sep 2021). Dried and ground needles were analyzed for starch and glucose content using the enzyme method (Landhäusser et al., 2018; Woodruff and Meinzer, 2011). Free glucose concentration was determined on a 96-well microplate photometer (Multiskan FC, Thermo Scientific) after enzymatic conversion to glucose-6-phosphate. Each sample was hydrolyzed by α-amylase and amyloglucosidase for starch. After enzymatic conversion to glucose-6-P, dehydrogenase was used to oxidize to gluconate-6-P. Glucose reference was used at 340 nm absorbance for photometric analysis. NSC concentrations are reported as % dry weight and proportion of glucose (=glucose/(glucose + starch)) and proportion of starch (=starch/(glucose + starch)).

Hydroscape area was determined based on (Meinzer et al., 2016). We completely withheld water during 13 Jul-9 Sep 2021 from a subset (n = 10 individuals per family, one family per species, Supporting Table S1) of potted individuals (separate from those used for all other measurements) and measured weekly predawn (~06 h00) and midday (~13 h00) leaf water potentials as individuals progressively dried out. To generate hydroscape area, we first plotted predawn leaf water potential (ψ_{pd}, x-axis) and midday leaf water potential (ψ_{md}, y-axis) and data points that were more negative than where $\psi_{pd} = \psi_{md}$ were removed (Supporting Figure S2). Then, starting where $\psi_{pd} = \psi_{md}$, points with less negative ψ_{pd} were iteratively added until the maximum r^2 for a linear fit of the linear regression between ψ_{pd} and ψ_{md} was reached. The y-intercept of this regression (ψ_{md} when $\psi_{pd} = 0$) was the predicted ψ_{md} under fully saturated soil and its intercept with the 1:1 line ($\psi_{pd} = \psi_{md}$) is the threshold at which stomatal closure is no longer effective in limiting ψ_{md} as ψ_{pd} becomes more negative. Finally, hydroscape area was determined as the area of the triangle produced by the regression line, the y-axis, and the 1:1 line in a plot of $\psi_{pd} = \psi_{md}$.

2.5. Photosynthetic-light and photosynthetic-CO_2 (A-C_i) response curves

Photosynthetic-light and –CO_2 response curves were measured on 30 Jul-25 Aug 2020 and 8 Jul-29 Jul 2020, respectively on fully expanded, mature needles on each of five individuals from each family using a portable photosynthesis instrument (LI-6800, Licor, Lincoln, NE USA). Cuvette conditions included a flow rate of 500 μmol s^{-1}, chamber pressure of 0.1 kPa, relative humidity of 60%, [CO_2] of 400 ppm, fan speed of 10,000 rpm, a leaf temperature of 25 °C, and a photosynthetic photon flux density (PPFD) of 1,600 μmol m^{-2} s^{-1}. For light response curves, C assimilation (A) was measured at each of the following photosynthetic photon flux density (PPFD) values: 2,400, 2,200, 2,000, 1,500, 1,200, 900, 600, 300, 150, 100, 50, and 0 μmol photons m^{-2} s^{-1} (Supporting Figure S3). We determined the following: A_{sat} (maximum photosynthetic rate in saturating light) was the maximum A on the plateau of the curve; Q_{sat} (light saturation point) was the PPFD value at A_{sat}; R_{dark} (respiration level under zero irradiance) was A at 0 PPFD; LCP (light compensation point) was the PPFD when $A = 0$, and QY (quantum yield) was the slope of the initial linear portion of the curve (Lambers and Oliveira, 2019). For A-C_i curves, A was measured at each of the following CO_2 values, in order: 400, 300, 200, 100, 50, 400, 400, 600, 800, 1,000, 1,200, 1,600, 2,000, 2,400, 2,800 ppm (Supporting Figure S4). We determined the following using the (Sharkey et al., 2007) tool: V_{cmax} (maximum velocity of Rubisco for carboxylation) was calculated as the initial slope of the curve; J_{max} (maximum rate of electron transport); R_{day} (day respiration rate) was calculated as the y-intercept of the initial linear portion of the curve; and A_{max} (maximum net assimilation rate) was determined as the maximum A value on the plateau of the A-C_i curve (e.g., (Manter et al., 2000; Meinzer et al., 2004)). After light response and A-C_i curves were completed, needles were collected, photographed, and analyzed in ImageJ to correct gas exchange values for leaf area.

2.6. Pressure-volume (P-V) curves

P-V curves were measured on a small shoot with mature, fully expanded foliage (at least 10 fascicles) from each of 5 individuals from each family during 15 May-10 Jun 2021. Shoots were excised before dawn, kept in the dark, placed in a sealed plastic bag containing a damp paper towel, transported to the lab, and rehydrated. We conducted the bench drying method (Meinzer et al., 2014; Tyree and Hammel, 1972) by making repeated measurements of shoot mass and water potential

(Ψ) using a pressure chamber (PMS Instruments, Corvallis, OR, USA) as the shoot dried out. P-V curves were plotted as 100-relative water content (%) on the x-axis and $-1/\Psi$ (MPa) on the y-axis (Supporting Figure S5), and were considered complete when 3–5 points were made along the linear portion of the P-V curve. Needles were photographed to determine fresh leaf area (analyzed with ImageJ), dried for 48 h at 70 °C, then weighed for dry mass. We determined the following: Ψ_{FT} (water potential at full turgor), Ψ_{TLP} (water potential at turgor loss point), ε (modulus of elasticity), RWC_{TLP} (relative water content at turgor loss point), C_{FT} (capacitance at full turgor), SWC (saturated water content), and α_f (apoplastic fraction).

2.7. Heat tolerance curves

Heat tolerance curves were measured using two methods: chlorophyll fluorescence and electrolyte leakage (EL) according to (Marias et al., 2017, 2016). Curves were measured on mature, fully expanded foliage of each of five individuals from each family from 18 to 21 Sep 2021. Four to ten fascicles per individual were collected before dawn, kept in the dark, sealed in a plastic bag containing a damp paper towel, transported to the lab, and stored at 4 °C until measurements were made (within 1 h).

For chlorophyll fluorescence curves, two needles per individual were placed in small, sealed plastic bags and were submerged in a preheated water bath for 15 min at each of seven temperatures: 35 °C, 40 °C, 45 °C, 50 °C, 55 °C, 60 °C, and 65 °C. Temperatures of the water bath and needles were confirmed with fine-wire thermocouples. After 15 min at each temperature, needles were stored in the dark for 24 h. Controls were not exposed to the water bath. Then, chlorophyll fluorescence (F_V/F_M, F_O) was measured using the fluorometer of a LI-6800 portable photosynthesis system. Fluorometer settings included: rectangular flash type, a dark modulation rate of 200 Hz for the measuring beam, red target of the flash set at 10,000 μmol m^{-2} s^{-1}, and a flash duration of 1,000 ms. F_V/F_M, the maximum quantum yield of photosystem II, was calculated as: $\frac{F_M-F_O}{F_M}=\frac{F_V}{F_M}$, where F_m represents maximum fluorescence, F_O represents minimal fluorescence, and F_V represents variable fluorescence. From plots of F_V/F_M and F_O vs temperature, T_{50} of F_V/F_M was calculated as the temperature at which 50% of maximum F_V/F_M is reduced. T_{crit} of F_O represents the temperature at which F_O begins to increase.

For EL curves, needles were cut transversely at their midpoint, placed in 6 mL of DI water in polycarbonate test tubes, placed in a vacuum desiccator for 15 min, and then placed in a preheated water bath for 20 min at each of 10 temperatures: 30 °C, 40 °C, 45 °C, 50 °C, 55 °C, 60 °C, 65 °C, 70 °C, 75 °C, and 80 °C. Water bath temperature was confirmed with fine-wire thermocouples and thermometer. After 20 min in the water bath, tubes were gently shaken for 30 min at 450 rpm and then electrical conductivity was measured with an Accumet™ AB200 Benchtop pH/Conductivity Meter (Thermo Fisher Scientific Inc., Waltham, MA). Controls were not exposed to the water bath. Tubes were then transferred to boiling water (100 °C) for 20 min, shaken for another 30 min at 450 rpm, and final conductivity was measured (100% electrolyte leakage). Percent EL (%EL) was calculated as: $\frac{C1}{C2}$*100, where C1 represents conductivity after exposure to the initial water bath temperature and C2 represents conductivity after exposure to 100 °C. %EL represents cellular membrane integrity and increases with increasing stress. From plots of %EL and temperature, T_{50} of EL ($T_{50\_}EL$) was calculated as the temperature where 50% EL occurred.

2.8. Cold tolerance curves

Cold tolerance curves were measured on mature, fully expanded foliage of each of five individuals from each family on 17–21 Aug 2021 using chlorophyll fluorescence and EL (similar to heat tolerance curves). Two needles were collected from each individual before dawn. For chlorophyll fluorescence curves, needles were placed in a glass vial with 0.5 mL DI water. For EL, needles were rinsed with DI water, cut into ten segments, and placed in a glass vial with 0.2 mL of DI water. Vials were placed in a programmable freezer (TUJR-A-F4T, Tenney Environmental, New Columbia, PA, USA) where the temperature started at 4 °C and then dropped by 4 °C hr^{-1} until the test temperature of −24 °C was reached. The test temperature of −24 °C was chosen from a range of test temperatures because it produced moderate levels of freezing damage. Temperature was held at −24 °C for one hour. Chlorophyll fluorescence curve samples thawed for 24 h at 4 °C and dark-adapted chlorophyll fluorescence (F_V/F_M) was measured with a fluorometer of a LI-6800 portable photosynthesis system. EL samples thawed for 2 h at 4 °C, had 3.3 mL of DI water added, incubated at 4 °C for 20 h, were shaken at 120 rpm for 30 mins at room temperature, and electrical conductivity was measured. Then, samples were placed in boiling water for 20 mins, shaken for another 30 mins, and final conductivity was measured. Percent EL was calculated as stated for heat tolerance.

2.9. Statistical analysis

All statistical analyses were conducted in R (v 2022.07.1). Linear mixed-effects models (*lme4*, *emmeans* packages) were used to evaluate the effect of species on each trait mean, using species as a fixed effect and family as a random effect to account for differences between families within species. For gas exchange (A, g_s) and NSC (starch, glucose) trait means, species was used as a fixed effect and week was used as a random effect to account for differences between measurement dates within species. Chi-squared significance values were determined at $p \leq 0.05$. P-values between 0.06 and 0.1 indicated marginal significance. Assumptions of normality and linearity were checked with residual plots. Values with Cooks distance values greater than 0.5 were considered influential and removed. Log transformations were used when needed to meet assumptions.

3. Results

Compared to PIAL, PIFL exhibited relatively greater acquisitive and conservative resource use traits that enabled PIFL's generalist strategy. PIFL's greater acquisitive resource use traits compared to PIAL included greater high-light tolerance (greater Q_{sat}, greater fascicle density, marginally lower STAR ($p = 0.061$), Fig. 2), higher biomass allocation to photosynthetic tissue (higher aboveground:belowground biomass, higher needle:branch + stem biomass, higher needle:branch biomass), earlier budburst phenology (fewer days to budburst stages 4, 5, and 6 but not stages 2 and 3; Fig. 3), and higher C and water uptake (greater stomatal pore area, stomatal pore length, stomatal density per length, stomatal density per area, stomatal density per volume; greater C assimilation rate) (Table 2, Fig. 4).

PIFL's greater conservative resource use traits compared to PIAL included greater physical stress resistance (higher stem base diameter, shorter stem height, higher stem base diameter:stem height, higher branch diameter, higher branch diameter:branch length, marginally shorter branch length ($p = 0.084$)), greater drought tolerance (higher SWC, higher leaf starch proportion, lower glucose proportion, lower glucose concentration, Fig. 3), and greater drought avoidance (earlier budburst phenology, smaller hydroscape area) (Table 2, Fig. 3, Supporting Figure S2).

The two species did not significantly differ in LMA, needle width, needle length, total biomass, branch + stem biomass, root biomass, stomatal pore length, g_s, starch concentration, leaf $\delta^{13}C$, and leaf N content (Supporting Information Table S2). The two species did not significantly differ in the following high-light tolerance traits: R_{dark}, QY, LCP, and A_{sat}, and drought tolerance traits: ψ_{FT}, ψ_{TLP}, ε, RWC_{TLP}, C_{FT}, and α_F. The two species did not significantly differ in any photosynthetic capacity, heat tolerance, or cold tolerance traits (Supporting Information Table S2).

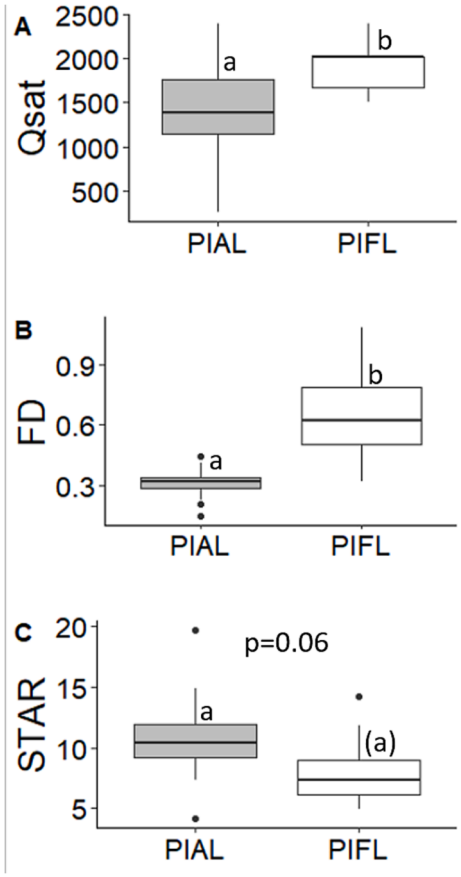

Fig. 2. PIFL (limber pine) exhibited greater high-light tolerance than PIAL (whitebark pine) via (A) significantly higher Q_{sat} (light saturation point, μmol m^{-2} s^{-1}, N = 10–20 per species), (B) higher FD (fascicle density, number of fascicles per mm of branch, N = 14–26 per species), and (C) lower STAR (sunlit leaf area to total leaf area ratio, N = 14–26 per species) than PIAL. Letters indicate significant differences between species means ($p \leq 0.05$, Table 2). Letters in parentheses indicate marginally significant differences between species means (p = 0.06–0.1).

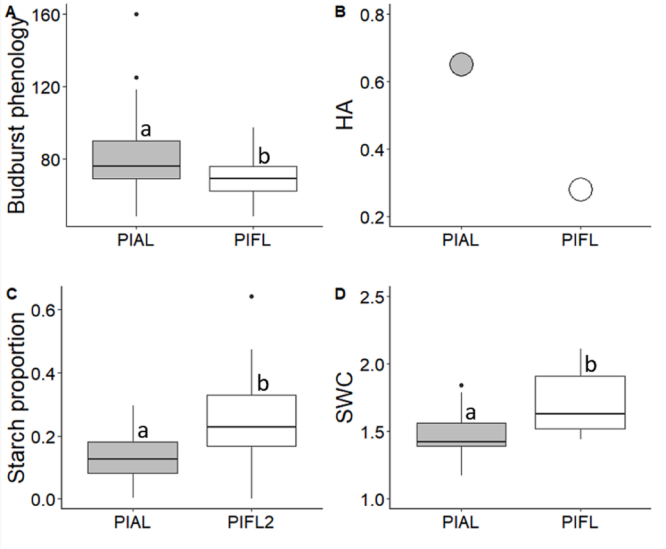

Fig. 3. PIFL (limber pine) exhibited greater drought avoidance than PIAL (whitebark pine) via (A) significantly earlier budburst phenology (number of days to budburst final stage 6, N = 50–77 per species) and (B) a smaller HA (hydroscape area, MPa^2, N = 10 per species) than PIAL. PIFL exhibited greater drought tolerance than PIAL via (C) higher starch proportion (starch/(glucose + starch), % dry weight, N = 10 per species) and (D) higher SWC (saturating water content, g water (g dry mass)$^{-1}$, N = 10–20 per species) than PIAL. Letters indicate significant differences between species means ($p \leq 0.05$, Table 2).

4. Discussion

Overall, our results suggest that PIFL's acquisitive and conservative resource use traits contribute to its generalist strategy and ability to inhabit a greater range of elevations than PIAL. PIFL may be better adapted to more high-light environments, may have higher C assimilation and water uptake, and may grow faster earlier in the season, respectively, than PIAL. This is suggested by PIFL's greater acquisitive and conservative resource use traits. PIFL's greater acquisitive traits included: greater high-light tolerance (greater Q_{sat}, greater fascicle density), biomass allocation to photosynthetic tissue (higher needle biomass, aboveground:belowground biomass, needle:branch + stem biomass), and C and water uptake (greater stomatal density and size, higher C assimilation rate). PIFL's greater conservative traits included: greater physical stress resistance (shorter height, higher stem and branch diameters, greater branch and stem diameter:length), drought tolerance (higher SWC, leaf starch proportion), and drought avoidance (earlier budburst phenology, smaller hydroscape area) than PIAL. PIFL may enable more efficient use of high-light loads and maximize CO_2 uptake when moisture is abundant during spring snowmelt before the onset of dry summer conditions (Letts et al., 2009). Other conservative resource use traits describing cold tolerance, heat tolerance, drought tolerance (some traits), and high-light tolerance (some traits) did not differ between species, suggesting that both species exhibit traits that promote similar conservative resource use enabling their overlapping persistence at higher elevations.

4.1. Generalist PIFL exhibits greater high-light tolerance, allocation to photosynthetic tissue, and physical stress resistance than specialist PIAL

PIFL demonstrated greater high-light tolerance than PIAL via greater Q_{sat}; greater fascicle density, shorter height, higher stem and branch diameters and greater branch and stem diameter:length; higher needle biomass, aboveground:belowground biomass, and needle:branch + stem biomass. These species differences suggest that PIFL may be more successful than PIAL at persisting in high-elevation environments with high sky exposure, common habitats for foundation species like PIFL and PIAL (Tomback et al., 2011). This high sky exposure results in high sunlight exposure, high daytime temperatures, low nighttime temperatures, and dew and frost formation (Körner, 2002). Greater Q_{sat} is a mechanism by which foliage may physiologically adjust to higher saturating light levels (Valladares and Niinemets, 2008). Greater fascicle density (i.e. needle clustering) and lower STAR are crown morphological adjustments that reduce harmful excess light absorption (Demmig-Adams and Adams, 1992) by increasing self-shading through overlapping branches and foliage (Germino and Smith, 1999). Lower STAR is observed in sun shoots compared to shade shoots (Oker-Blom and Smolander, 1988). Lower STAR, needle clustering (i.e. greater fascicle density), and PIFL's shorter stature may also reduce low temperature photoinhibition by reducing convective heat dissipation foliage (Germino and Smith, 1999). This short stature and dense crown architecture coincided with PIFL's higher needle biomass, which was supported by thicker diameter branches and stems compared to PIAL, together contributing to increased self-shading (Gerrish, 1990) and increased capacity to withstand windy environments, snow load, or herbivory (Read and Stokes, 2006). Compared to PIAL, PIFL's greater high-light tolerance, allocation to photosynthetic tissue, and physical stress resistance may enable higher conservative resource use to better establish at upper treeline (bright, windy environments), as well as higher acquisitive resource use to better compete with other species at lower

Table 2
Whitebark pine (PIAL) and limber pine (PIFL) mean trait values that significantly differed between species ($p < 0.05$). Traits that did not significantly differ between species are presented in Supporting Table S2. SE = standard error, df = degrees of freedom, Chisq = Chi-squared value, N = sample size per species. Units listed below each trait.

Type	Trait		PIAL	PIFL	P-value	Chisq	N
Crown morphology	Fascicle density (FD)	Mean	0.307	0.662	1.8E-09	36.22	14–26
	# fascicles mm^{-1}	SE	0.0495	0.0422			
		df	3.7	0.86			
	Stem base diameter	Mean	0.726	0.841	0.04512	4.01	14–26
	cm	SE	0.0483	0.0412			
		df	3.7	0.86			
	Stem height	Mean	15.1	11.6	0.00014	14.46	14–26
	cm	SE	0.687	0.646			
		df	3.1	1.73			
	Stem base diameter:Stem height	Mean	0.0471	0.0733	0.00037	12.67	14–26
		SE	0.00569	0.00513			
		df	3.16	1.53			
	Branch diameter	Mean	2.78	3.43	0.01893	5.51	14–26
	mm	SE	0.233	0.199			
		df	3.7	0.86			
	Branch diameter:Branch length	Mean	0.0701	0.157	0.00020	13.79	14–26
		SE	0.0186	0.0163			
		df	3.26	1.35			
	STAR (sunlit leaf area:Total leaf area)	Mean	11.01	8.08	0.06072	3.52	14–26
		SE	1.2	1.09			
		df	3.24	1.61			
Biomass	Needle biomass	Mean	7.65	11.64	0.02825	4.8127	14–26
	(g)	SE	1.5	1.29			
		df	4.14	1.17			
	Aboveground:belowground biomass	Mean	1.46	2.38	0.00132	10.31	14–26
		SE	0.21	0.209			
		df	4.11	1.87			
	Needle:Branch + stem biomass	Mean	1.36	2.2	0.00244	9.19	14–26
		SE	0.194	0.206			
		df	4.18	2.13			
	Needle:Branch biomass	Mean	1.68	2.96	0.00179	9.75	14–26
		SE	0.288	0.305			
		df	4.18	2.12			
Stomatal	Stomatal pore size (area)	Mean	270	304	0.00314	8.72	20–36
	μm^2	SE	6.93	9.17			
		df	3.95	3.44			
	Stomatal density per length	Mean	0.0121	0.0141	1.7E-07	27.29	20–36
	# stomata mm^{-1}	SE	0.000232	0.000319			
		df	3.94	4.18			
	Stomatal density per area	Mean	16.4	19.8	0.00029	13.16	20–36
	# stomata mm^{-2}	SE	0.579	0.785			
		df	3.9	4.12			
	Stomatal density per volume	Mean	22.9	28.7	0.0240	5.09	20–36
	# stomata mm^{-3}	SE	1.54	2.09			
		df	3.92	4.15			
Budburst phenology	# days to budburst stage 4	Mean	59.2	46.1	0.0006	11.78	50–77
		SE	2.38	3.04			
		df	3.46	3.32			
	# days to budburst stage 5	Mean	75.4	57.4	8.3E-06	19.87	50–77
		SE	2.65	3.17			
		df	3.35	2.68			
	# days to budburst stage 6	Mean	80.0	67.8	0.0002	13.6	50–77
		SE	2.23	2.46			
		df	4.01	2.31			
Physiological	*A* (C assimilation rate)	Mean	3.87	5.56	0.00601	7.55	3–5
	$\mu mol\ m^{-2}\ s^{-1}$	SE	0.537	0.556			
		df	52.7	52.7			
	Starch proportion (Starch/(Gluc + Starch))	Mean	0.135	0.249	0.00813	7.00	3–5
	% dry weight	SE	0.0418	0.0404			
		df	5.88	5.12			
	Glucose	Mean	0.277	0.14	5.0E-06	20.84	3–5
	% dry weight	SE	0.0225	0.0212			
		df	10	8.08			
	Glucose proportion (Gluc/(Gluc + Starch))	Mean	0.865	0.751	0.00813	7.00	3–5
	% dry weight	SE	0.0418	0.0404			
		df	5.88	5.12			
	Hydroscape area	Mean	0.65	0.28	NA	NA	5–10
	MPa^2	SE	NA	NA			
		df	NA	NA			
High-light tolerance	Q_{sat} (light saturation point)	Mean	1447	1872	0.03235	4.58	5–15
	$\mu mol\ m^{-2}\ s^{-1}$	SE	112	166			
		df	3.64	4.56			

(*continued on next page*)

Table 2 (*continued*)

Type	Trait		PIAL	PIFL	P-value	Chisq	N
Drought tolerance	SWC (saturating water content) g water (g dry mass)$^{-1}$	Mean	1.48	2.33	0.03941	4.24	5–15
		SE	0.238	0.339			
		df	3.41	4.53			

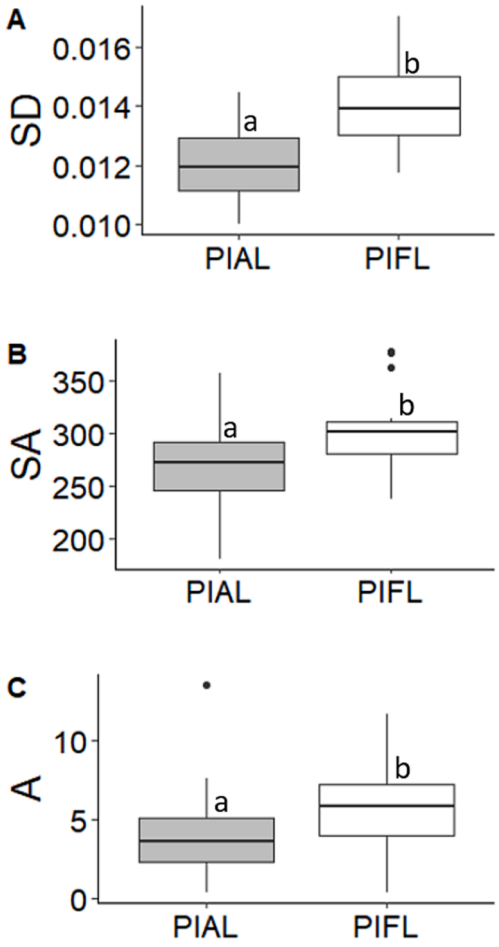

Fig. 4. PIFL (limber pine) exhibited greater C and water uptake than PIAL (whitebark pine) via (A) significantly higher SD (stomatal density, number of stomatal per length in mm, N = 20–36 per species), (B) higher SA (stomatal pore area, μm^2, N = 20–36 per species), and (C) higher A (C assimilation rate, μmol m^{-2} s^{-1}, N = 3–5 per species) than PIAL. Letters indicate significant differences between species means ($p \leq 0.05$, Table 2).

elevations.

4.2. Generalist PIFL exhibits earlier budburst phenology than specialist PIAL

PIFL's earlier budburst compared to PIAL may enable PIFL to avoid peak summer drought, consistent with field observations of PIFL maximizing gas exchange during the spring and fall, while minimizing gas exchange during summer (Letts et al., 2009). Earlier budburst may enable higher acquisitive C and water use early in the season and higher conservative C and water use during summer drought, together contributing to PIFL being a superior pioneer and generalist than PIAL. PIFL's earlier budburst may occur because the risk of early season frost-induced injury (Hänninen and Tanino, 2011) is lower since PIFL often inhabits lower elevations that are warmer, resulting in earlier, more rapid snowmelt. In contrast, PIAL's later budburst timing may reflect PIAL inhabiting higher elevations where low temperatures and frozen soil limit photosynthesis and water availability (Tranquillini, 1982) and where the risk of cold injury due to early spring frost is higher than for PIFL. PIAL's later budburst also may reduce the risk of frost desiccation (Tranquillini, 1982). Frost desiccation is defined as increasing desiccation of plants during winter when transpiration continues because of high irradiation, leaf heating, and increased evaporative demand but uptake of water is limited because of soils and stems remain frozen (Körner, 1999). Additionally, PIAL's later budburst timing may coincide with its more northern and higher elevation distribution where temperatures are cooler, and juveniles may be snow-covered longer compared to PIFL. For example, longer snow cover of dwarf pine (*P. mugo*) delayed post-winter recovery in springtime photochemical efficiency compared to cembran pine (*Pinus cembra*) (Lehner and Lütz, 2003). Consistently, we hypothesize that photosynthesis of PIFL may recover faster from winter dormancy due to less time covered by snow via earlier budburst timing and higher high-light tolerance than PIAL. Snow cover protects evergreen conifers from stressful low temperatures and high light intensities (Sakai and Larcher, 1987; Tranquillini, 1982). This may help explain why we found no significant differences in cold tolerance between species, despite PIAL having a more northern and higher elevation distribution. PIFL's earlier budburst than PIAL may promote both conservative and acquisitive resource use, characteristics previously observed in generalists (Sanaphre-Villanueva et al., 2017). Earlier budburst especially under warming temperatures may extend tree growing seasons and compensate for reduced C uptake during dry periods (Grossiord et al., 2022); however, the consequences of earlier spring budburst phenology on total annual C uptake especially under future warming in high-elevation conifer species requires further investigation.

4.3. Generalist PIFL exhibits higher C and water uptake, drought tolerance, and drought avoidance than specialist PIAL

PIFL's greater stomatal size and stomatal density are consistent with PIFL's greater high-light tolerance and consistent with other studies that have observed increases in stomatal density with increasing irradiance to enhance photosynthetic capacity (Poorter et al., 2019) through increased CO_2 uptake (Yamori et al., 2020). Stomatal density has been negatively related to stomatal size (Hetherington and Woodward, 2003) but this negative relationship between stomatal density and stomatal size is not observed at smaller guard cell lengths of 0–25 um. Accordingly, we did not observe a negative relationship between stomatal density and stomatal size as stomatal pore length was 22.4 μm and 23.3 μm for PIAL and PIFL, respectively (Table 2). PIAL's stomatal density was similar to that measured in (Bennett et al., 2018). PIAL's smaller, fewer stomata than PIFL may reduce the size and number of entry points for non-native fungal pathogen white pine blister rust (*C. ribicola*) (Patton and Johnson, 1970), which may be advantageous to PIAL given that heritable major gene resistance to white pine blister rust has been identified in PIFL (dominant R gene named *Cr4*), but not in PIAL (Schoettle et al., 2014).

Because plants can regulate the sensitivity, speed, and timing (e.g., daily and seasonal timescales) of stomatal opening and closure in response to dynamic environmental conditions, these dynamic traits may more strongly determine operating pore area, plant water loss, CO_2 uptake, and intrinsic water use efficiency than relatively static traits like stomatal size and density alone (Drake et al., 2013; Lawson and Vialet-Chabrand, 2019). Consistently, despite observing significantly greater stomatal density and stomatal size in PIFL than PIAL, we did not observe

significant species differences in leaf $\delta^{13}C$, suggesting that traits related to stomatal regulation (e.g. stomatal sensitivity, kinetics), rather than stomatal density, determine overall intrinsic water use efficiency (A/g_s), derived from leaf $\delta^{13}C$ (Goodrich et al., 2016). This is also important to consider since higher stomatal size and stomatal density alone may appear to lower drought tolerance (Davies et al., 1974). We did, however, observe significantly higher rates of A (but not g_s) in PIFL than PIAL, suggesting that A/g_s increased on a shorter time scale (vs a longer time-integrated metric of water use efficiency like $\delta^{13}C$). Accordingly, based on hydroscape area, a stomatal sensitivity trait, PIFL appears to be relatively more isohydric and therefore more drought avoidant while PIAL appears to be relatively more anisohydric and therefore more drought tolerant. Isohydric species have exhibited slower stomatal opening and activation of photosynthesis than relatively anisohydric species (Meinzer et al., 2017). This is consistent with PIFL's larger stomata that also tend to have slower stomatal kinetics (Drake et al., 2013). Faster stomatal kinetics may be advantageous under dry and/or variable conditions by buffering transpiration-induced changes in xylem tension and balancing efficient water supply and xylem damage due to embolism (Brodribb et al., 2017). However, relatively isohydric PIFL may not rely on faster stomatal kinetics to respond to changing drought conditions because PIFL may avoid summer drought altogether by exhibiting high sensitivity to high VPD (Letts et al., 2009) and maximizing photosynthesis in the spring (exhibited by our observed earlier budburst phenology) and fall seasons while minimizing gas exchange in summer (Letts et al., 2009). This drought avoidance strategy may contribute to our observed lack of significant species differences in traits typically correlated with drought tolerance (e.g., LMA (Poorter et al., 2009; Wright et al., 2005), turgor loss point (Bartlett et al., 2012)). However, PIFL did exhibit significantly higher SWC, which may increase water storage to buffer against and avoid drought (Sapes et al., 2019), and also a higher proportion of leaf starch (concurrent with lower glucose proportion and lower glucose concentration), observed to increase drought survival (Woodruff et al., 2015). PIFL's higher C and water uptake (greater stomatal density and size, higher C assimilation rate), drought tolerance (higher SWC, leaf starch proportion, lower glucose proportion, lower glucose concentration), and drought avoidance (earlier budburst phenology, smaller hydroscape area) demonstrate both higher acquisitive and conservative resource use (Sanaphre-Villanueva et al., 2017), supporting its generalist strategy compared to PIAL.

4.4. Conclusions

Our results reveal mechanisms underlying: species establishment and survival, the contribution of juvenile physiology to PIAL and PIFL's contrasting elevational distributions, and the observation of PIFL as a generalist and PIAL as a specialist. PIFL exhibited both acquisitive and conservative resource use traits that contribute to its generalist strategy and ability to inhabit a greater range of elevations than PIAL. PIAL and PIFL did not differ in conservative resource use traits describing cold tolerance, heat tolerance, drought tolerance (some traits), and high-light tolerance (some traits), suggesting that both species have traits that promote similar conservative resource use enabling their overlapping persistence at higher elevations. Together, our results suggest that PIFL's greater high-light tolerance, increased biomass allocation to photosynthetic tissue, higher C and water uptake, greater physical stress resistance, and higher drought tolerance and drought avoidance than PIAL, may make PIFL better adapted to more high-light environments, maximize C assimilation when water is available, and grow faster earlier in the season than PIAL. PIFL's possible drought avoidance of maximizing gas exchange earlier in the growing season may make the species well-suited to persist during future warmer, drier conditions in the western US (Letts et al., 2009). Certain combinations of traits may determine differences in survival and persistence in these marginal habitats (Germino and Smith, 1999) and can improve our understanding of how species distributions will be affected by changing climates. This will enable us to develop management strategies to decrease forest vulnerability and increase adaptive capacities under future climates (Chmura et al., 2011). In this study, we focused on how seedling traits may contribute to contrasting elevational distributions and generalist-specialist strategies. However, we acknowledge that other abiotic and biotic factors such as competition and soil type can influence seedling establishment and species distributions. Therefore, future work comparing whitebark pine and limber pine should explicitly investigate other such factors.

CRediT authorship contribution statement

Danielle E.M. Ulrich: Conceptualization, Data curation, Formal analysis, Investigation, Methodology, Writing – original draft, Writing – review & editing. **Chloe Wasteneys:** Conceptualization, Data curation, Formal analysis, Investigation, Methodology, Writing – review & editing. **Sean Hoy-Skubik:** Conceptualization, Data curation, Formal analysis, Investigation, Methodology, Writing – review & editing. **Franklin Alongi:** Conceptualization, Data curation, Formal analysis, Investigation, Methodology, Writing – review & editing.

Declaration of Competing Interest

The authors declare that they have no known competing financial interests or personal relationships that could have appeared to influence the work reported in this paper.

Data availability

Data are available at the Dryad Digital Repository: https://doi.org/10.5061/dryad.bzkh189dm.

Acknowledgements

Thanks to Kelly Kerr, Charlotte Grossiord, and Brian Smithers for helpful feedback on early manuscript drafts. Thanks to the US Forest Service Coeur d'Alene Nursery for plant material. Thanks to Katherine Sparks, Meghan McFadden, Rachael Robbins, Jade Berghoff, Jack Tierney, Jessie Irish, Jaime Henriquez, Robert Beers, Oskar Robinson, Brian Smithers, David Baumbauer, and MSU's Plant Growth Center greenhouse for help with pine care and measurements. This work was supported by MSU's Ecology Department, MSU's Undergraduate Scholars program, US Forest Service Forest Health Protection (grant number 19-JV-11221637-180), Whitebark Pine Ecosystem Foundation, Montana Native Plant Society, and Sitka Gear.

Appendix A. Supplementary data

Supplementary data to this article can be found online at https://doi.org/10.1016/j.foreco.2023.121113.

References

Ackerly, D.D., Loarie, S.R., Cornwell, W.K., Weiss, S.B., Hamilton, H., Branciforte, R., Kraft, N.J.B., 2010. The geography of climate change: implications for conservation biogeography. Divers. Distrib. 16, 476–487. https://doi.org/10.1111/j.1472-4642.2010.00654.x.

Adams, H.D., Macalady, A.K., Breshears, D.D., Allen, C.D., Stephenson, N.L., Saleska, S. R., Huxman, T.E., 2010. Climate-induced tree mortality: Earth system consequences. Eos Trans. Am. Geophys. Union 91 (17), 153.

Allen, C.D., Macalady, A.K., Chenchouni, H., Bachelet, D., McDowell, N., Vennetier, M., Kitzberger, T., Rigling, A., Breshears, D.D., Hogg, E.H., Gonzalez, P., Fensham, R., Zhang, Z., Castro, J., Demidova, N., Lim, J.-H., Allard, G., Running, S.W., Semerci, A., Cobb, N., 2010. A global overview of drought and heat-induced tree mortality reveals emerging climate change risks for forests. For. Ecol. Manag. 259 (4), 660–684. https://doi.org/10.1016/j.foreco.2009.09.001.

Arno, S.F., 1989. Silvics of whitebark pine (Pinus albicaulis). US Department of Agriculture, Forest Service, Intermountain Research Station.

Bartlett, M.K., Scoffoni, C., Sack, L., 2012. The determinants of leaf turgor loss point and prediction of drought tolerance of species and biomes: a global meta-analysis. Ecol. Lett. 15, 393–405.
Bennett, P., Hill, J., Savin, D.P., Kegley, A., Schoettle, A., Sniezko, R.A., Bird, B., Stone, J., 2018. Genetic variation in stomate densities and needle traits in a rangewide sampling of whitebark Pine (Pinus albicaulis). Schoettle Anna W Sniezko Richard Kliejunas John T Eds Proc. IUFRO Jt. Conf. Genet. Five-Needle Pines Rusts For. Trees Strobusphere 2014 June 15-20 Fort Collins CO Proc RMRS-P-76 Fort Collins CO US Dep. Agric. For. Serv. Rocky Mt. Res. Stn. P 30-40 76, 30–40.
Borgman, E.M., Schoettle, A.W., Angert, A.L., 2015. Assessing the potential for maladaptation during active management of limber pine populations: a common garden study detects genetic differentiation in response to soil moisture in the Southern Rocky Mountains. Can. J. For. Res. 45 (4), 496–505.
Bradley St Clair, J., Howe, G.T., 2007. Genetic maladaptation of coastal Douglas-fir seedlings to future climates. Glob. Change Biol. 13, 1441–1454. https://doi.org/10.1111/j.1365-2486.2007.01385.x.
Brodribb, T.J., McAdam, S.A., Carins Murphy, M.R., 2017. Xylem and stomata, coordinated through time and space. Plant Cell Environ. 40, 872–880. https://doi.org/10.1111/pce.12817.
Chmura, D.J., Anderson, P.D., Howe, G.T., Harrington, C.A., Halofsky, J.E., Peterson, D. L., Shaw, D.C., Clair, J.B.S., 2011. Forest responses to climate change in the northwestern United States: ecophysiological foundations for adaptive management. For. Ecol. Manag. 261 (7), 1121–1142.
Cleaver, C.M., Jacobi, W.R., Burns, K.S., Means, R.E., 2017. Limber pine regeneration and white pine blister rust in the central and southern rocky mountains. For. Sci. 63, 151–164. https://doi.org/10.5849/forsci.16-052.
COSEWIC, 2010. Committee on the Status of Endangered Wildlife in Canada (COSEWIC) Assessment and Status Report on the Whitebark Pine (Pinus albicaulis) in Canada.
COSEWIC, 2014. Committee on the Status of Endangered Wildlife in Canada (COSEWIC) Assessment and Status Report on the Limber Pine (Pinus flexilis) in Canada.
Davies, W.J., Kozlowski, T.T., Lee, K.J., 1974. Stomatal characteristics of pinusresinosa and pinusstrobus in relation to transpiration and antitranspirant efficiency. Can. J. For. Res. 4, 571–574. https://doi.org/10.1139/x74-086.
Demmig-Adams, B., Adams, W.W., 1992. Photoprotection and other responses of plants to high light stress. Annu. Rev. Plant Physiol. Plant Mol. Biol. 43 (1), 599–626.
Drake, P.L., Froend, R.H., Franks, P.J., 2013. Smaller, faster stomata: scaling of stomatal size, rate of response, and stomatal conductance. J. Exp. Bot. 64, 495–505.
Germino, M.J., Smith, W.K., 1999. Sky exposure, crown architecture, and low-temperature photoinhibition in conifer seedlings at alpine treeline. Plant Cell Environ. 22 (4), 407–415.
Gernandt, D.S., López, G.G., García, S.O., Liston, A., 2005. Phylogeny and classification of Pinus. TAXON 54 (1), 29–42. https://doi.org/10.2307/25065300.
Gerrish, G., 1990. Relating carbon allocation patterns to tree senescence in metrosideros forests. Ecology 71, 1176–1184. https://doi.org/10.2307/1937385.
Goeking, S.A., Izlar, D.K., 2018. Pinus albicaulis Engelm. (Whitebark Pine) in mixed-species stands throughout Its US range: broad-scale indicators of extent and recent decline. Forests 9, 131. https://doi.org/10.3390/f9030131.
Goodrich, B.A., Waring, K.M., Kolb, T.E., Tognetti, R., 2016. Genetic variation in *Pinus strobiformis* growth and drought tolerance from southwestern US populations. Tree Physiol. 36 (10), 1219–1235.
Grossiord, C., Bachofen, C., Gisler, J., Mas, E., Vitasse, Y., Didion-Gency, M., 2022. Warming may extend tree growing seasons and compensate for reduced carbon uptake during dry periods. J. Ecol. 110, 1575–1589. https://doi.org/10.1111/1365-2745.13892.
Hankin, L.E., Bisbing, S.M., 2021. Let it snow? Spring snowpack and microsite characterize the regeneration niche of high-elevation pines. J. Biogeogr. 48, 2068–2084. https://doi.org/10.1111/jbi.14136.
Hänninen, H., Tanino, K., 2011. Tree seasonality in a warming climate. Trends Plant Sci. 16, 412–416. https://doi.org/10.1016/j.tplants.2011.05.001.
Hansen, A.J., East, A., Keane, R.E., Lavin, M., Legg, K., Holden, Z., Toney, C., Alongi, F., 2021. Is whitebark pine less sensitive to climate warming when climate tolerances of juveniles are considered? For. Ecol. Manag. 493, 119221 https://doi.org/10.1016/j.foreco.2021.119221.
Hetherington, A.M., Woodward, F.I., 2003. The role of stomata in sensing and driving environmental change. Nature 424, 901–908. https://doi.org/10.1038/nature01843.
IPCC [WWW Document], 2018. IPCC 2018 Spec. Rep. Glob. Warm. 15C. URL https://www.ipcc.ch/sr15/.
Jacobs, J., Weaver, T., 1990. Effects of temperature and temperature preconditioning on seedling performance of whitebark pine. Gen. Tech. Rep. INT USA.
Johnson, D.M., McCulloh, K.A., Reinhardt, K., 2011. The Earliest Stages of Tree Growth: Development, Physiology and Impacts of Microclimate. In: Meinzer, F.C., Lachenbruch, B., Dawson, T.E. (Eds.), Size- and Age-Related Changes in Tree Structure and Function, Tree Physiology. Springer, Netherlands, pp. 65–87.
Keane, R.E., Holsinger, L.M., Mahalovich, M.F., Tomback, D.F., 2017. Restoring whitebark pine ecosystems in the face of climate change. Gen Tech Rep RMRS-GTR-361 Fort Collins CO US Dep. Agric. For. Serv. Rocky Mt. Res. Stn. 123 P 361.
Körner, C., 1999. Alpine plant life: functional plant ecology of high mountain ecosystems.
Körner, C., 2002. Impact of atmospheric changes on high mountain vegetation, in: Mountain Environments in Changing Climates. Routledge, pp. 149–157.
Lambers, H., Oliveira, R.S., 2019. Plant Physiological Ecology, 3rd ed. Springer International Publishing. https://doi.org/10.1007/978-3-030-29639-1.
Landhäusser, S.M., Chow, P.S., Dickman, L.T., Furze, M.E., Kuhlman, I., Schmid, S., Wiesenbauer, J., Wild, B., Gleixner, G., Hartmann, H., Hoch, G., McDowell, N.G., Richardson, A.D., Richter, A., Adams, H.D., Mencuccini, M., 2018. Standardized protocols and procedures can precisely and accurately quantify non-structural carbohydrates. Tree Physiol. 38 (12), 1764–1778. https://doi.org/10.1093/treephys/tpy118.
Lawson, T., Vialet-Chabrand, S., 2019. Speedy stomata, photosynthesis and plant water use efficiency. New Phytol. 221, 93–98. https://doi.org/10.1111/nph.15330.
Lehner, G., Lütz, C., 2003. Photosynthetic functions of cembran pines and dwarf pines during winter at timberline as regulated by different temperatures, snowcover and light. J. Plant Physiol. 160, 153–166. https://doi.org/10.1078/0176-1617-00798.
Letts, M.G., Nakonechny, K.N., Van Gaalen, K.E., Smith, C.M., 2009. Physiological acclimation of *Pinus flexilis* to drought stress on contrasting slope aspects in Waterton Lakes National Park, Alberta, Canada. Can. J. For. Res. 39, 629–641. https://doi.org/10.1139/X08-206.
Mahalovich, M.F., Kimsey, M.J., Fortin-Noreus, J.K., Robbins, C.T., 2016. Isotopic heterogeneity in whitebark pine (*Pinus albicaulis* Engelm.) nuts across geographic, edaphic and climatic gradients in the Northern Rockies (USA). For. Ecol. Manag. 359, 174–189. https://doi.org/10.1016/j.foreco.2015.09.047.
Maher, E.L., Germino, M.J., Hasselquist, N.J., 2005. Interactive effects of tree and herb cover on survivorship, physiology, and microclimate of conifer seedlings at the alpine tree-line ecotone. Can. J. For. Res. 35, 567–574. https://doi.org/10.1139/x04-201.
Manter, D.K., Bond, B.J., Kavanagh, K.L., Rosso, P.H., Filip, G.M., 2000. Pseudothecia of Swiss needle cast fungus, Phaeocryptopus gaeumannii, physically block stomata of Douglas fir, reducing CO_2 assimilation. New Phytol. 148, 481–491. https://doi.org/10.1046/j.1469-8137.2000.00779.x.
Marias, D.E., Meinzer, F.C., Woodruff, D.R., McCulloh, K.A., 2016. Thermotolerance and heat stress responses of Douglas-fir and ponderosa pine seedling populations from contrasting climates. Tree Physiol. 37, 301–315. https://doi.org/10.1093/treephys/tpw117.
Marias, D.E., Meinzer, F.C., Still, C., 2017. Impacts of leaf age and heat stress duration on photosynthetic gas exchange and foliar nonstructural carbohydrates in *Coffea arabica*. Ecol. Evol. 7, 1297–1310. https://doi.org/10.1002/ece3.2681.
Martínez-Berdeja, A., Hamilton, J.A., Bontemps, A., Schmitt, J., Wright, J.W., 2019. Evidence for population differentiation among Jeffrey and *Ponderosa pines* in survival, growth and phenology. For. Ecol. Manag. 434, 40–48. https://doi.org/10.1016/j.foreco.2018.12.009.
Meinzer, F.C., Woodruff, D.R., Shaw, D.C., 2004. Integrated responses of hydraulic architecture, water and carbon relations of western hemlock to dwarf mistletoe infection. Plant Cell Environ. 27 (7), 937–946.
Meinzer, F.C., Woodruff, D.R., Marias, D.E., Mcculloh, K.A., Sevanto, S., 2014. Dynamics of leaf water relations components in co-occurring iso- and anisohydric conifer species. Plant Cell Environ. 37, 2577–2586. https://doi.org/10.1111/pce.12327.
Meinzer, F.C., Woodruff, D.R., Marias, D.E., Smith, D.D., McCulloh, K.A., Howard, A.R., Magedman, A.L., Penuelas, J., 2016. Mapping 'hydroscapes' along the iso-to anisohydric continuum of stomatal regulation of plant water status. Ecol. Lett. 19 (11), 1343–1352.
Meinzer, F.C., Smith, D.D., Woodruff, D.R., Marias, D.E., McCulloh, K.A., Howard, A.R., Magedman, A.L., 2017. Stomatal kinetics and photosynthetic gas exchange along a continuum of isohydric to anisohydric regulation of plant water status. Plant Cell Environ. 40, 1618–1628. https://doi.org/10.1111/pce.12970.
Monahan, W.B., Cook, T., Melton, F., Connor, J., Bobowski, B., Lamb, E.G., 2013. Forecasting distributional responses of limber pine to climate change at management-relevant scales in rocky mountain national park. PLoS One 8 (12), e83163. https://doi.org/10.1371/journal.pone.0083163.
Oker-Blom, P., Smolander, H., 1988. The ratio of shoot silhouette area to total needle area in Scots in pine. For. Sci. USA.
Overton, E., Park, J., Robertson, N., Eramian, A., 2016. Current practices for growing Whitebark Pine seedlings at the U.S. Department of Agriculture, Forest Service, Coeur d'Alene Nursery. Tree Plant. Notes 59, 64–68.
Patton, R.F., Johnson, D.W., 1970. Mode of penetration of needles of eastern white pine by *Cronartium ribicola*. Phytopathology 60, 977–982.
Poorter, H., Niinemets, Ü., Poorter, L., Wright, I.J., Villar, R., 2009. Causes and consequences of variation in leaf mass per area (LMA): a meta-analysis. New Phytol. 182 (3), 565–588.
Poorter, H., Niinemets, Ü., Ntagkas, N., Siebenkäs, A., Mäenpää, M., Matsubara, S., Pons, T., 2019. A meta-analysis of plant responses to light intensity for 70 traits ranging from molecules to whole plant performance. New Phytol. 223, 1073–1105. https://doi.org/10.1111/nph.15754.
PRISM [WWW Document], 2018. PRISM Clim. Group Or. State Univ. URL http://prism.oregonstate.edu.
Read, J., Stokes, A., 2006. Plant biomechanics in an ecological context. Am. J. Bot. 93, 1546–1565. https://doi.org/10.3732/ajb.93.10.1546.
Reich, P.B., Cornelissen, H., 2014. The world-wide 'fast–slow'plant economics spectrum: a traits manifesto. J. Ecol. 102 (2), 275–301.
Reinhardt, K., Castanha, C., Germino, M.J., Kueppers, L.M., Pereira, J., 2011. Ecophysiological variation in two provenances of *Pinus flexilis* seedlings across an elevation gradient from forest to alpine. Tree Physiol. 31 (6), 615–625.
Sakai, A., Larcher, W., 1987. Low Temperature and Frost as Environmental Factors. In: Sakai, A., Larcher, W. (Eds.), Frost Survival of Plants: Responses and Adaptation to Freezing Stress, Ecological Studies. Springer, Berlin, Heidelberg, pp. 1–20. https://doi.org/10.1007/978-3-642-71745-1_1.
Sanaphre-Villanueva, L., Dupuy, J.M., Andrade, J.L., Reyes-García, C., Jackson, P.C., Paz, H., 2017. Patterns of plant functional variation and specialization along secondary succession and topography in a tropical dry forest. Environ. Res. Lett. 12 (5), 055004. https://doi.org/10.1088/1748-9326/aa6baa.
Sapes, G., Roskilly, B., Dobrowski, S., Maneta, M., Anderegg, W.R.L., Martinez-Vilalta, J., Sala, A., 2019. Plant water content integrates hydraulics and carbon depletion to

predict drought-induced seedling mortality. Tree Physiol. 39, 1300–1312. https://doi.org/10.1093/treephys/tpz062.
Savolainen, O., Pyhäjärvi, T., Knürr, T., 2007. Gene flow and local adaptation in trees. Annu. Rev. Ecol. Evol. Syst. 38, 595–619. https://doi.org/10.1146/annurev.ecolsys.38.091206.095646.
Schneider, C.A., Rasband, W.S., Eliceiri, K.W., 2012. NIH Image to ImageJ: 25 years of image analysis. Nat. Methods 9 (7), 671–675.
Schoettle, A.W., Sniezko, R.A., 2007. Proactive intervention to sustain high-elevation pine ecosystems threatened by white pine blister rust. J. For. Res. 12 (327–336), 327–336.
Schoettle, A.W., Sniezko, R.A., Kegley, A., Burns, K.S., 2014. White pine blister rust resistance in limber pine: evidence for a major gene. Phytopathology 104 (2), 163–173.
Sharkey, T.D., Bernacchi, C.J., Farquhar, G.D., Singsaas, E.L., 2007. Fitting photosynthetic carbon dioxide response curves for C3 leaves. Plant Cell Environ. 30, 1035–1040.
Steele, R., 1990. *Pinus flexilis* James limber pine. Silv. N. Am. 1, 348–354.
Tomback, D.F., Achuff, P., Schoettle, A.W., Schwandt, J.W., Mastrogiuseppe, R.J., 2011. The magnificent high-elevation five-needle white pines: Ecological roles and future outlook. Keane Robert E Tomback Diana F Murray Michael P Smith Cyndi M Eds Future High-Elev. Five-Needle White Pines West. N. Am. Proc. High Five Symp. 28-30 June 2010 Missoula MT Proc. RMRS-P-63 Fort Collins CO US Dep. Agric. For. Serv. Rocky Mt. Res. Stn. P 2-28 63, 2–28.
Tranquillini, W., 1982. Frost-Drought and Its Ecological Significance. In: Lange, O.L., Nobel, P.S., Osmond, C.B., Ziegler, H. (Eds.), Physiological Plant Ecology II: Water Relations and Carbon Assimilation, Encyclopedia of Plant Physiology. Springer, Berlin, Heidelberg, pp. 379–400. https://doi.org/10.1007/978-3-642-68150-9_12.
Tyree, M.T., Hammel, H.T., 1972. The measurement of the turgor pressure and the water relations of plants by the pressure-bomb technique. J. Exp. Bot. 23 (1), 267–282.
U.S. Fish and Wildlife Service, 2022. Endangered and Threatened Wildlife and Plants; Threatened Species Status With Section 4(d) Rule for Whitebark Pine (Pinus albicaulis).
Valladares, F., Niinemets, Ü., 2008. Shade tolerance, a key plant feature of complex nature and consequences. Annu. Rev. Ecol. Evol. Syst. 39, 237–257. https://doi.org/10.1146/annurev.ecolsys.39.110707.173506.
Vogan, P.J., Schoettle, A.W., 2015. Selection for resistance to white pine blister rust affects the abiotic stress tolerances of limber pine. For. Ecol. Manag. 344, 110–119. https://doi.org/10.1016/j.foreco.2015.01.029.
Woodruff, D.R., Meinzer, F.C., 2011. Water stress, shoot growth and storage of non-structural carbohydrates along a tree height gradient in a tall conifer. Plant Cell Environ. 34, 1920–1930.
Woodruff, D.R., Meinzer, F.C., Marias, D.E., Sevanto, S., Jenkins, M.W., McDowell, N.G., 2015. Linking nonstructural carbohydrate dynamics to gas exchange and leaf hydraulic behavior in *Pinus edulis* and *Juniperus monosperma*. New Phytol. 206, 411–421. https://doi.org/10.1111/nph.13170.
Wright, I.J., Reich, P.B., Westoby, M., Ackerly, D.D., Baruch, Z., Bongers, F., Cavender-Bares, J., Chapin, T., Cornelissen, J.H.C., Diemer, M., Flexas, J., Garnier, E., Groom, P.K., Gulias, J., Hikosaka, K., Lamont, B.B., Lee, T., Lee, W., Lusk, C., Midgley, J.J., Navas, M.-L., Niinemets, Ü., Oleksyn, J., Osada, N., Poorter, H., Poot, P., Prior, L., Pyankov, V.I., Roumet, C., Thomas, S.C., Tjoelker, M.G., Veneklaas, E.J., Villar, R., 2004. The worldwide leaf economics spectrum. Nature 428, 821–827. https://doi.org/10.1038/nature02403.
Wright, I.J., Reich, P.B., Cornelissen, J.H.C., Falster, D.S., Groom, P.K., Hikosaka, K., Lee, W., Lusk, C.H., Niinemets, Ü., Oleksyn, J., Osada, N., Poorter, H., Warton, D.I., Westoby, M., 2005. Modulation of leaf economic traits and trait relationships by climate. Glob. Ecol. Biogeogr. 14, 411–421. https://doi.org/10.1111/j.1466-822x.2005.00172.x.
Yamori, W., Kusumi, K., Iba, K., Terashima, I., 2020. Increased stomatal conductance induces rapid changes to photosynthetic rate in response to naturally fluctuating light conditions in rice. Plant Cell Environ. 43, 1230–1240. https://doi.org/10.1111/pce.13725.